polymers

MDPI

Article

Development of Biodegradable Composites Using Polycaprolactone and Bamboo Powder

Satya Guha Nukala [1], Ing Kong [1,*], Vipulkumar Ishvarbhai Patel [1], Akesh Babu Kakarla [1], Wei Kong [2] and Oliver Buddrick [3]

[1] School of Computing, Engineering and Mathematical Sciences, La Trobe University, Bendigo, VIC 3550, Australia
[2] Centre for Foundation and General Studies, Infrastructure University Kuala Lumpur, Block 11, De Centrum City, Jalan Ikram-Uniten, Kajang 43000, Selangor, Malaysia
[3] Faculty of Higher Education, William Angliss Institute, Melbourne, VIC 3000, Australia
* Correspondence: i.kong@latrobe.edu.au

Abstract: The use of biodegradable polymers in daily life is increasing to reduce environmental hazards. In line with this, the present study aimed to develop a fully biodegradable polymer composite that was environmentally friendly and exhibited promising mechanical and thermal properties. Bamboo powder (BP)-reinforced polycaprolactone (PCL) composites were prepared using the solvent casting method. The influence of BP content on the morphology, wettability, and mechanical and thermal properties of the neat matrix was evaluated. In addition, the degradation properties of the composites were analysed through soil burial and acidic degradation tests. It was revealed that BP contents had an evident influence on the properties of the composites. The increase in the BP content has significantly improved the tensile strength of the PCL matrix. A similar trend is observed for thermal stability. Scanning electron micrographs demonstrated uniform dispersion of the BP in the PCL matrix. The degradation tests revealed that the biocomposites with 40 wt·% of BP degraded by more than 20% within 4 weeks in the acidic degradation test and more than 5% in the soil burial degradation test. It was noticed that there was a considerable difference in the degradation between the PCL matrix and the biocomposites of PCL and BP. These results suggest that biodegradable composites could be a promising alternative material to the existing synthetic polymer composites.

Keywords: bamboo powder; polycaprolactone; biodegradable; mechanical properties; thermal properties; hardness

Citation: Nukala, S.G.; Kong, I.; Patel, V.I.; Kakarla, A.B.; Kong, W.; Buddrick, O. Development of Biodegradable Composites Using Polycaprolactone and Bamboo Powder. *Polymers* **2022**, *14*, 4169. https://doi.org/10.3390/polym14194169

Academic Editor: Grażyna Adamus

Received: 9 August 2022
Accepted: 26 September 2022
Published: 4 October 2022

1. Introduction

The use of products made from polymers in the daily lives of individuals and society has increased due to their ease of production and relatively low cost and versatility [1,2]. However, this increase has led to the accumulation of an enormous amount of polymeric waste, which poses a serious hazard to the environment. Notably, most polymeric products are developed from non-biodegradable polymers, which can take years to degrade at the end of the product life cycle [3]. Therefore, researchers have been actively seeking ways to reduce the environmental impacts of polymeric products through the practice of reducing, reusing, and recycling [4,5]. Thus, there is a glowing interest in exploiting new eco-friendly materials based on biodegradable polymers to reduce environmental hazards [6].

Biodegradable polymers are materials that can degrade in the environment when exposed to various conditions such as temperature, ultraviolet radiation, humidity, and soil pH [7]. In addition, other ecological actions involving microorganisms (bacteria, fungi, and algae) aid the rapid degradation of polymers. As a result, biodegradable polymers can be transformed into water, carbon dioxide, or methane gas without causing environmental

pollution [8]. Polycaprolactone (PCL) is a notable biodegradable polymer that can be obtained through the polymerisation of hydroxy caproic acid or by opening the ϵ-caprolactone ring [9]. PCL has good mechanical properties, such as flexibility and impact resistance [10], low glass transition and melting temperatures [11], and biocompatibility. Furthermore, PCL can degrade easily in a short period (a few months to many years), depending on its molecular weight, degree of crystallinity, shape, porosity, and the surrounding environment [12]. Therefore, PCL is used in numerous products, such as packaging materials, microcapsules for sustainable agriculture, and biomedical orthopedic applications [13]. The cost and complexity of the PCL manufacturing process greatly limit its large-scale applications.

One of the effective and economic methods to reduce the production cost of PCL is to partially replace the expensive polymer with low-cost fillers without sacrificing the biodegradation performance of PCL. Karakus et al. [14] studied the thermal and mechanical properties of PCL reinforced with wheat straw flour composites. The composites were produced by using the injection moulding technique. Adding wheat straw flour to the PCL matrix improved the flexural and tensile modulus but reduced the impact strength and elongation at break. Valdés et al. [15] evaluated the morphological, mechanical, thermal, and degradation properties of PCL-based biocomposites reinforced with almond skin. The results indicated that an increase of filler loading from 10 wt·% to 30 wt·% increases the elastic modulus from 280 MPa to 350 MPa. The improved thermal properties with increased filler content indicated effective adhesion between the matrix and filler. Furthermore, the presence of almond skin in PCL aided in accelerating the degradation rate of composites.

Bamboo is one of the most rapidly growing species of timber material. It possesses strong mechanical and thermal properties, and it has low nitrogen, sulphur, and ash content. According to Kitagawa et al. [16], 60% of the cellulose found in bamboo has a high concentration of lignin. Furthermore, bamboo has a small microfibrillar angle (2–10°). Because of these intrinsic properties, bamboo has been widely used in many applications such as fencing, furniture, roofing, clothing, and especially in construction and scaffolding in the construction industry. The high consumption of bamboo has led to the accumulation of waste bamboo in landfills. This sustainable waste material can be reused in the production of composites as reinforcement for various polymer matrices. Researchers have developed a range of methods to extract bamboo in the form of fibers, particulates, and powders [17–19].

Rasheed et al. [20] developed biodegradable composites with microcrystalline cellulose (MCC) extracted from bamboo chips reinforced with polylactic acid (PLA) and polybutylene succinate (PBS). The biocomposites were produced by melt-mixing at 180 °C and hot-pressing at 180 °C. The results stated that the addition of MCC enhanced the crystallinity, thermal stability, and tensile strength of the PLA-PBS blends. Xing et al. [21] studied the effect of the bamboo flour (BF) loading on the mechanical properties, thermal stability and, melt-crystallisation behaviour of a blend of PCL and PLA. BF-reinforced PCL-PLA composites were manufactured by blending BF and PCL–PLA using the melt-mixing process. The results revealed that the mechanical properties of composites first increased and then decreased with the increase in BF loading. The further impact strength, tensile, and elongation at the break of the composites achieved a maximum of 1.26 kJ/m^2, 12.68 MPa, and 5.2%, respectively, when the BF mass fraction was 40%. There were no significant changes in the thermal properties with the increase in the BF mass fraction, although a change in the glass transition temperature and an increase in the crystallisation temperature were identified [21]. Chen et al. [22] examined the mechanical and rheological properties of PLA-polypropylene (PP) reinforced with bamboo fibers. The composites demonstrated a uniform dispersion of bamboo fibers in the matrix. Furthermore, the thermal and mechanical properties were strengthened when the filler loading was increased by up to 35%. Qi et al. [23] investigated a bamboo powder (BP)-reinforced PBS composite as a biofilm carrier for denitrification. The results indicated that the incorporation of BP in a PBS matrix achieved the acceptable removal of nitrates. An antibacterial analysis demonstrated

that the interaction between the composite and bacterial and fungal communities played a vital role in composite degradation and denitrification.

Many studies focused on developing a novel material by mixing biodegradable polymers with natural fibers [24,25]. However, the open literature has provided very little attention to the combination of PCL and waste products of bamboo. Therefore, in this study, the bamboo powder was extracted from the waste products of bamboo after industrial processing and used as a filler to reinforce the PCL matrix. The composites were characterised using a scanning electron microscope (SEM) and Fourier transform infrared (FTIR) spectroscopy to observe the morphological and chemical interactions of the composites. In addition, the influence of bamboo powder on the thermal and mechanical properties of the PCL matrix is also analysed. Furthermore, the porosity, wettability, and biodegradability of the composites were assessed.

2. Materials and Methods

2.1. Materials

PCL, dichloromethane (DCM), and hydrochloric acid (HCl) were purchased from Sigma Aldrich (Melbourne, Australia), and the processed bamboo canes were supplied by Raw Boards Pty Ltd. (Bendigo, Australia). The canes were ground into a fine powder of 70–90 µm using a carpentry grinder.

2.2. Solvent Casting and Compression Moulding

Initially, the BP was dried in the oven at 105 °C for 24 h to remove the moisture content. Subsequently, PCL and BP were weighed according to the weight percentage, as summarised in Table 1 [10]. The PCL was then dissolved in the DCM through mechanical stirring at a temperature of 50 °C and a speed of 500 rpm for 1 h, and the BP was slowly added to the solution, stirred for another 30 min to achieve a mixing consistency, and finally, the mixture was poured into a petri dish and oven dried at 40 °C for 24 h. The composite film was then peeled off from the petri dish and broken into small fragments and compressed using a hydraulic hot press at a temperature of 60 °C and a pressure of 20 kPa for 15 min. The illustration of the solvent casting of PCL-BP composites is shown in Figure 1.

Table 1. Composition of PCL-BP composites.

Composite	PCL (wt·%)	BP (wt·%)
PCL	100	0
PCL-BP10	90	10
PCL-BP20	80	20
PCL-BP30	70	30
PCL-BP40	60	40

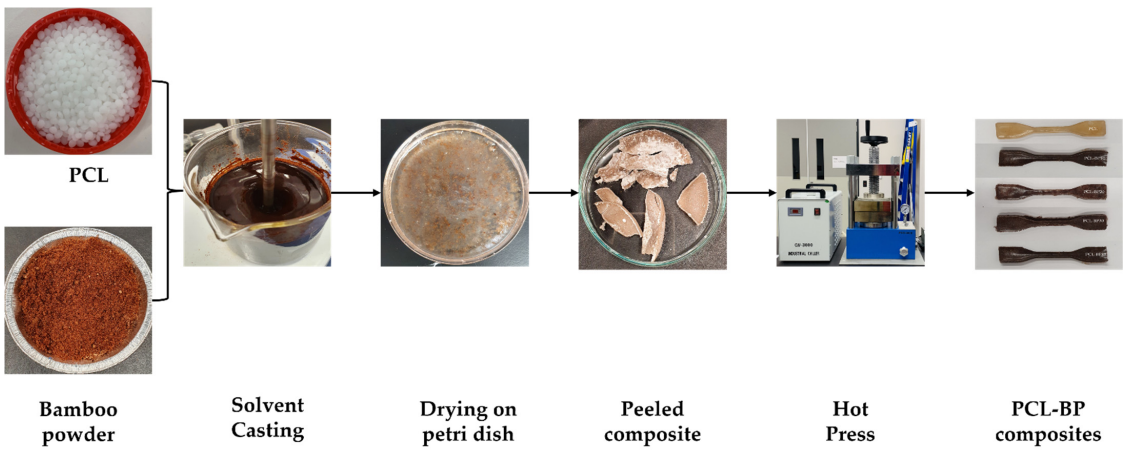

Figure 1. Illustration of the solvent casting of PCL and PCL-BP composites.

2.3. Morphology

The morphology of the fractured cross-sectional surface of the PCL-BP composites was observed using an SEM (Hitachi Benchtop SEM 3030, Tokyo, Japan). The samples were vacuum sputter coated with platinum at 10 kV for 30 s before the microstructure was examined. The micrographs were obtained at 15 kV in a low vacuum mode.

2.4. Degradation

2.4.1. Soil Burial Degradation

The PCL-BP composites were buried in wet fertile black soil for the soil biodegradation test [26]. The black soil consisted of hummus, which included crushed tree branches and leaves. The test was carried out at room temperature, and the relative humidity was 70–90%. The samples (5 cm in length) were buried in loose soil under the top-soil surface layer and weighed at regular intervals of 4, 8, 12, 16, 20, 24, and 28 days. The samples were washed with distilled water to remove any residual dirt and oven dried at 50 °C to measure weight loss [27,28]. Each composite was weighed before and after degradation, and the weight loss of each composite was calculated using Equation (1):

$$M(\%) = \left[\left(M_i - M_f\right)/M_f\right] \times 100 \quad (1)$$

where M_i is the initial weight of the composite and M_f is the final weight of the composite.

2.4.2. Acidic Degradation

The PCL-BP composites were subjected to acidic degradation to evaluate their degradation in an acidic environment [26]. The degradation test was conducted in a glass bottle with a sample immersed in 50 mL of HCl. The sample was weighed at regular intervals of 2, 4, 6, 8, 10, 12, 14, 16, 18, 20, 22, 24, 26, and 28 days, and the average weight loss was calculated using Equation (2):

$$W(\%) = [(W_t - W_o)/W_o] \times 100 \quad (2)$$

where W_t and W_o are the specimen weights before and after immersion in acid, respectively. Each sample was performed thrice, and the mean and standard deviation (SD) were reported.

2.5. Porosity

The porosity percentage of the PCL-BP composites was evaluated based on Archimedes' principle using a specific gravity bottle [29,30]. The porosity of the composites was calculated based on Equation (3):

$$Porosity(P\%) = \frac{w_2 - w_3 - w_s/\rho_e}{w_1 - w_s/\rho_e} \times 100 \quad (3)$$

where w_1 is the specific gravity bottle weight filled with ethanol, w_2 is the specific gravity bottle weight with ethanol and sample, w_3 is the specific gravity bottle weight after the ethanol-saturated sample has been removed, w_s is the sample weight, and ρ_e is the ethonal density. Each sample was performed thrice, and the mean and standard deviation (SD) were reported.

2.6. Water Contact Angle Measurement

The contact angle of the PCL-BP composites was measured using the sessile-drop technique. A micrometre syringe was used to displace a droplet on the surface of the PCL-BP composites, and the contact angle was measured by scanning the droplet profile for 15 s with an Attention Theta Flex instrument (Biolin Scientific, Gothenburg, Sweden), following the procedure used in other studies [31,32]. The water droplet size was maintained at approximately 3 µL to avoid the effects of weight [33]. The measurements were repeated three times (n = 3) for each sample.

2.7. Thermal Analysis

2.7.1. Thermogravimetric Analysis

A thermogravimetric analysis (TGA) was performed using a PerkinElmer TGA 4000 (Waltham, MA, USA). Samples of approximately 4 mg were heated from 30 °C to 850 °C at a rate of 10 °C/min under a nitrogen flow of 20 mL/min.

2.7.2. Differential Scanning Calorimetry

Differential scanning calorimetry (DSC) measurements were performed using a PerkinElmer DSC 6000 (Waltham, MA, USA). First, the samples were heated from 30 °C to 200 °C at a rate of 20 °C/min and then retained at that temperature for 5 min to remove the thermal history. The samples were then cooled to 30 °C at a rate of 20 °C/min and heated again to 200 °C at a rate of 20 °C/min. The endothermic peaks were recorded as the enthalpy of melting (ΔH_m) and melting temperature (T_m).

2.8. Fourier Transform Infrared Spectroscopy

The FTIR spectra of the PCL-BP composites were recorded from 4000 to 650 cm^{-1} with the help of a computerised FTIR (Cary 630, Agilent Technologies, Santa Clara, CA, USA). The samples had been air-dried before the analysis. The transmission method used 32 scans with a 4 cm^{-1} resolution [34].

2.9. Mechanical Properties

2.9.1. Tensile Properties

The tensile properties of the composites were measured using a Zhongli ZL-8001A universal testing machine (Dongguan Zhongli Instrument Technology Co., Ltd., Dongguan, China) at a crosshead speed of 3 mm/min and a load of 500 kN, with the samples compressed using a hot press into dog-bone shape (ASTM D638 Type 4). The samples were in dry condition before testing and were tested at room temperature. Each sample was performed thrice, and the mean and standard deviation (SD) were reported.

2.9.2. Flexural Properties

The three-point bending behaviour of the PCL-BP composites was determined through three-point flexural testing using an Instron 5890 (Norwood, MA, USA) universal testing machine. The test was performed at 5% deflection of the composite samples [35,36]. The samples were prepared using hot press according to ASTM standards (ASTM D790) [37].

2.10. Hardness Test

The hardness test was conducted using Vickers hardness (DuraScan 32 series G5, Emco-Test, Kuchl, Austria). A 0.2 HV Vickers indenter was used to perform the measurement. Initially, a minor load of 5 kg was applied to ensure that the indenter penetrated the specimen, eliminating possible surface roughness errors. A major load of 10 kg was then applied for 10 s, and the hardness value was denoted in HV. The measurements were repeated three times (n = 3) for each sample.

2.11. Statistical Analysis

Statistical analysis was evaluated using GraphPad Prism 9.0 (GraphPad Software, Inc., San Diego, CA, USA) using the ANOVA method. The calculations were carried out three times (n = 3) for each sample and presented as mean ± standard deviation (SD) unless otherwise stated. The standard error of the mean is represented by error bars in all the figures, and the significance level of the p-value of ≤ 0.05 was determined to be significant (*). The analysis was performed based on the following literature [29,38,39].

3. Results and Discussion

3.1. Morphology

The SEM micrographs of BP and PCL-BP composites are presented in Figure 2. BP exhibited a rough surface (Figure 2a), which would help it to enhance the bonding between fiber and matrix [6]. In Figure 2b, the hot-pressed PCL showed a smooth and homogenous appearance. In addition, the stretch marks corresponded to the rupture of the specimen during the tensile test. Similar morphology was observed by Da Silva et al. [40]. Figure 2c,d shows the PCL-BP30 and PCL-BP40 composites, and it is evident that the BP was randomly dispersed in the PCL matrix [41]. In spite of the random dispersion of the BP, the PCL-BP composite exhibited some pores, as depicted in Figure 2e,f, which was evaluated using the porosity of the composite. Figure 2g,h depicts the energy dispersive X-ray (EDX) spectra of PCL and PCL-BP40. The carbon (C) and oxygen (O) peaks were expected to originate from the elemental composition of PCL. In the case of the PCL-BP40 composite, peaks of C and O were present, along with slight traces of sodium, potassium, chlorine, and silicon. The presence of the other elements may be caused by the contamination of the solvent during the solvent casting and hot-press procedures [34].

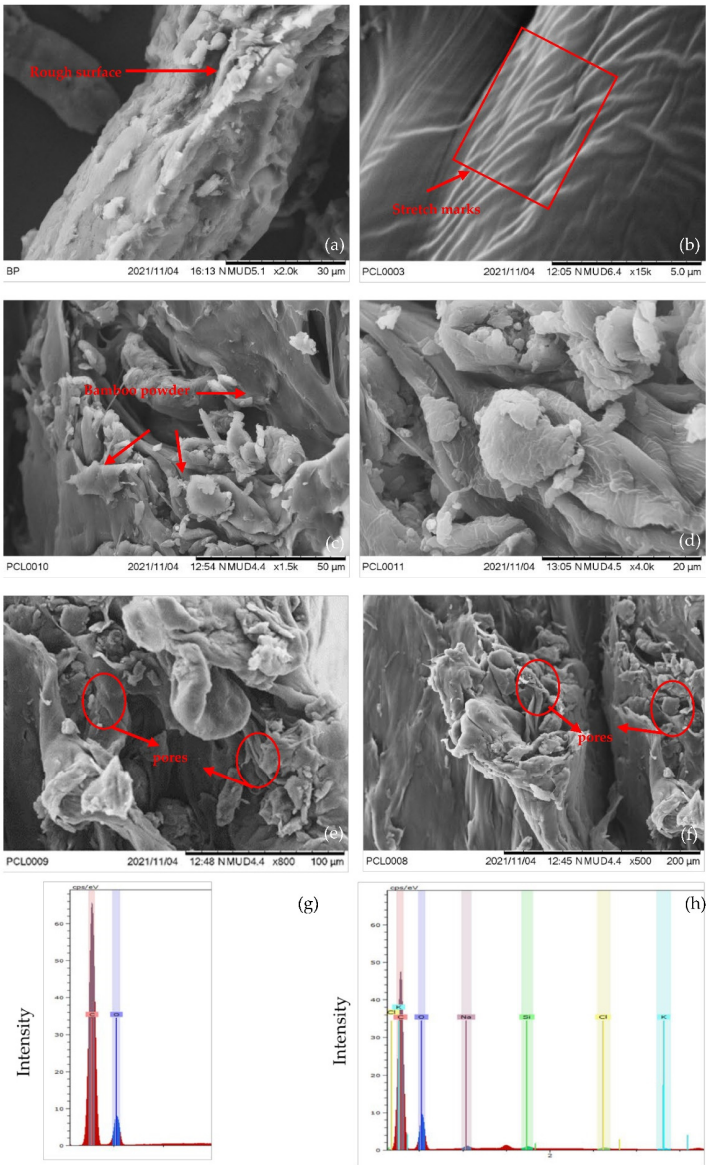

Figure 2. SEM micrographs of (**a**) BP; (**b**) PCL; (**c**) PCL-BP30; (**d**) PCL-BP40; (**e**) pores of PCL-BP30; (**f**) pores of PCL-BP40; EDX spectra of (**g**) PCL and (**h**) PCL-B40.

3.2. Fourier Transform Infrared Spectroscopy

The FTIR spectra of the PCL and PCL-BP composites are presented in Figure 3. In the spectra of PCL, the weak peaks observed at 2940 cm^{-1} and 2870 cm^{-1} corresponded to asymmetric elongation of the methylene-oxygen (CH_2-O) and symmetric methylene groups (CH_2), respectively [42,43]. The sharp and strong peak representing C=O bonds was observed at 1720 cm^{-1} [44]. Furthermore, the peaks at 1292 cm^{-1} were related to the stretching of the C-C and C-O bonds in the crystalline phase [45]. In addition, the peaks at 1165 cm^{-1} and 959 cm^{-1} correspond to the C-O-C bond and stretching of the oxime bond in PCL [43]. In the spectrum of the PCL-BP composite, an absorption band was observed at 3350–3250 cm^{-1}, which was assigned to typical OH stretching vibrations due to the contributions from -OH groups of the BP [46,47]. It can also be seen that when the BP content decreased, the band weakened [45,46]. Moreover, the peaks in the spectra of PCL-BP were similar to those of PCL, implying that there were no major structural changes due to the addition of BP in PCL, such as new chemical bond formation between the PCL chains and BP [43,48]. These spectra are consistent with those reported by Si et al. [11] and Vidal et al. [49].

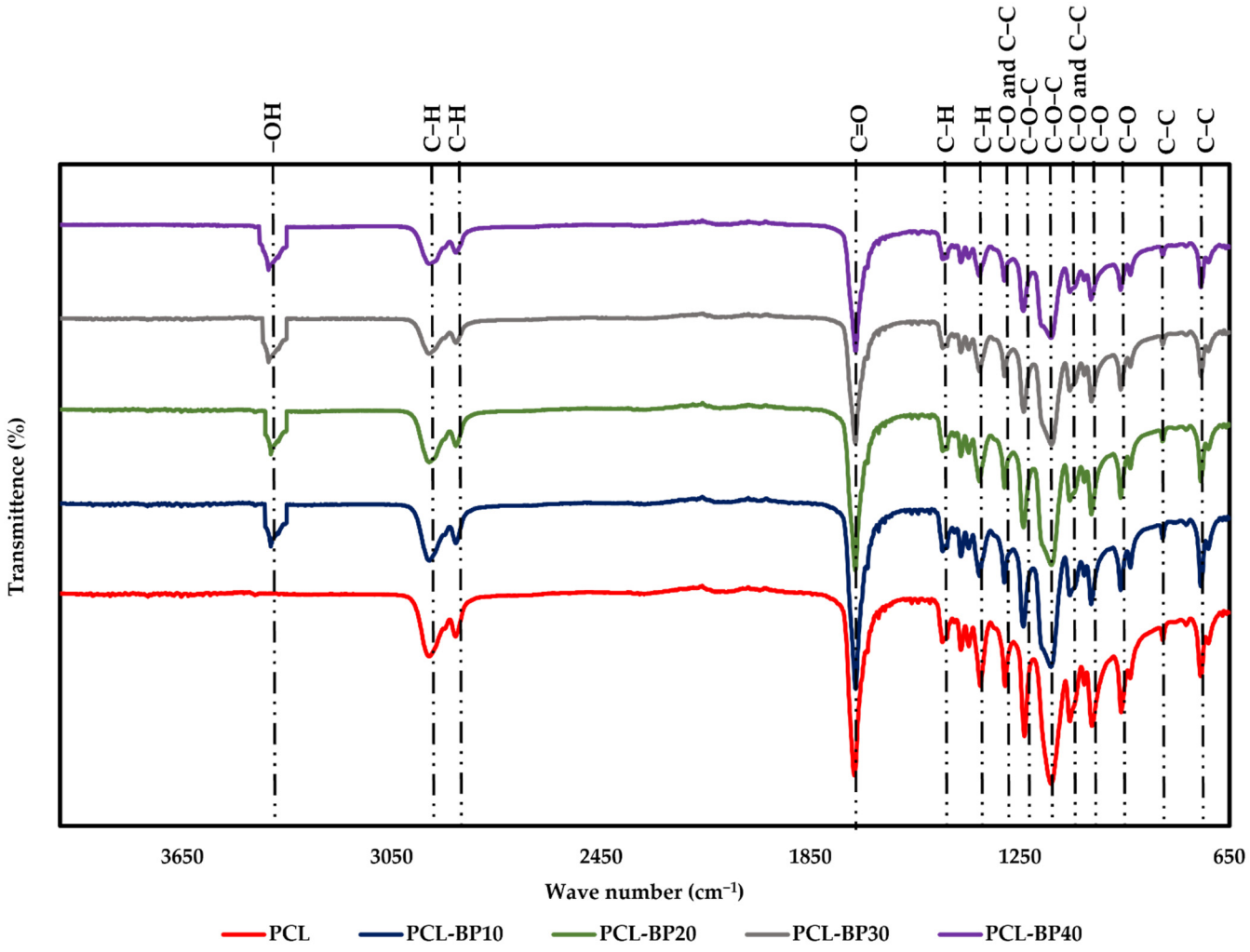

Figure 3. FTIR spectra of PCL and PCL-BP composites.

3.3. Porosity

The porosity of the PCL-BP composites is depicted in Figure 4. It can be seen from the figure that the increase in weight percentage of the BP increased the porosity of the PCL-BP composites. PCL had the lowest porosity at 0.41%, while the porosity of the PCL-BP composites increased from 1.3% to 3.25% with the increase of BP content from 10 wt·%

to 40 wt·%. The increase in porosity is due to the reduction in the overall density of the composites with the increase in BP content. Swain et al. [50] reported that the incorporation of natural fibers into a biodegradable polymer led to an increase in water absorption, which directly affected the porosity of the composites. This is because the natural fibers mainly consist of cellulose, hemicellulose, lignin, and other natural proteins, which have high water-retaining capacities [51], and hence, more water-absorbing pores can be formed.

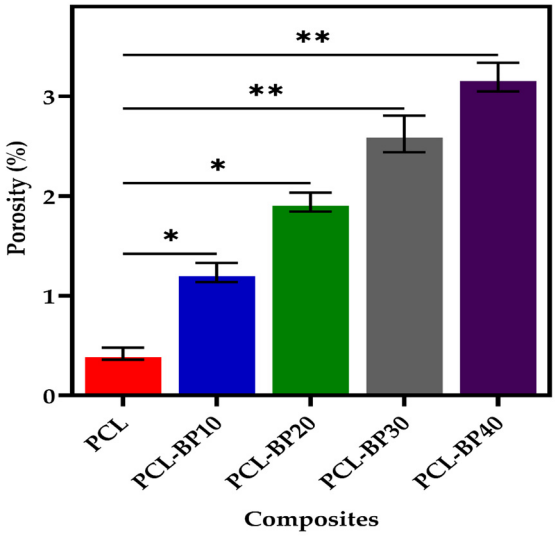

Figure 4. The porosity of PCL and PCL-BP composites (n = 3, * $p \leq 0.05$, ** $p \leq 0.01$).

3.4. Water Contact Angle

Figure 5a–e presents the sessile drop images on the composite surfaces to evaluate the water contact angle, and Figure 5f illustrates the contact angle measurements of PCL-BP composites. According to the literature, a contact angle below 90° indicates a good wetting surface for any liquids [52,53]. Figure 5 summarises the results, with the PCL surface having a water contact angle averaging approximately 65.33°, indicating partial wetting [54]. The water contact angle measurements for PCL-BP10 were 64.96°, followed by 59.58° for PCL-BP20, 56.18° for PCL-BP30, and 42.93°, the lowest water contact angle, for PCL-BP40. With the addition of BP, the water contact angle decreased due to the hydrophilic nature of BP. Wu et al. [55] studied the wettability of bamboo fiber-reinforced PLA composites. It was found that the contact angle decreased with the increase in bamboo fiber content in the composite. This could be due to the hydrophilicity of the bamboo fiber, which plays a vital role in decreasing the contact angles. The present study depicts a similar result as mentioned in the literature [55].

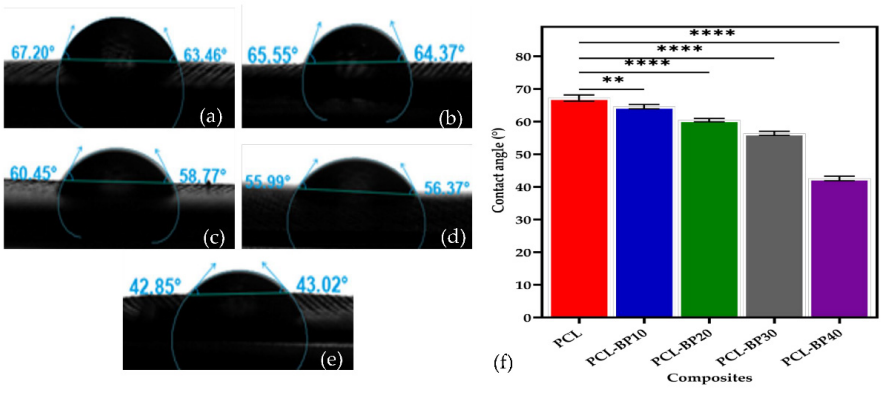

Figure 5. Sessile drop images of the PCL and its composites; (**a**) PCL; (**b**) PCL-BP10; (**c**) PCL-BP20; (**d**) PCL-BP30; (**e**) PCL-BP40; and (**f**) the contact angle measurements (n = 3, ** $p \leq 0.01$, **** $p \leq 0.0001$).

3.5. Degradation

3.5.1. Acidic Degradation

The acidic degradation and composites of PCL are presented in Figure 6. The composites were subjected to acidic degradation for 28 days. The degree of PCL weight loss increased with the number of days. In terms of the composites, PCL-BP40 degraded the most, followed by PCL-BP30, PCL-BP20, PCL-BP10, and PCL. It can be observed that the degree of weight loss increased with the increase in BP content over the same period. PCL showed the least weight loss, ranging up to 2.9% throughout the acidic degradation test period, whereas PCL-BP40 showed the highest degradation, with 20.5% of weight loss after 28 days of immersion in an acidic medium. It was followed by PCL-BP30, PCL-BP20, and PCL-BP10 showing weight losses of around 16.5%, 12.2%, and 7.3%, respectively. It was reported by Yang et al. [26] and Abdul Khalil et al. [6] that the BP contains certain chemical contents such as some amount of starch and many hydroxyl groups, which are very hydrophilic in nature. This hydrophilic nature of BP possesses a strong degradation ability when immersed in an acidic medium. The degradation studies were carried out according to Khalil et al. [6]. As a result of the increase in BP, the degradation of the composites increased, as noted in the studies by Dinesh et al. [56], Lyu et al. [43], and Schrip et al. [57].

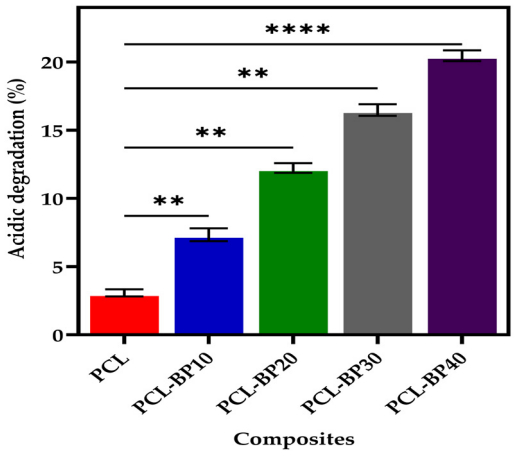

Figure 6. Acidic degradation of PCL and PCL-BP composites after 28 days of immersion in acidic medium (n = 3, ** $p \leq 0.01$, **** $p \leq 0.0001$).

3.5.2. Soil Burial Degradation

The biodegradation of the composites during the soil burial period occurred because of the presence of moisture and other enzymatic actions involving microorganisms, leading to the weight loss of the composite material [28]. Figure 7 represents the weight change of the PCL and its composites after they were subjected to soil burial degradation for 28 days. The weight loss of the composites was more significant than expected with the increase in soil burial time. Higher loadings of BP led to greater weight loss after 28 days. Among all the composites, PCL-BP40 demonstrated the highest biodegradability, with 5.1% of weight loss after 28 days of soil burial. PCL-BP30, PCL-BP20, and PCL-BP10 demonstrated weight losses of 4.5%, 3.9%, and 3.5%, respectively, after 28 days of soil burial. However, the weight loss of the pure PCL was minimal, ranging up to 0.6% throughout the soil burial test period. The chemical contents, such as cellulose, hemicellulose, and lignin, and the hygroscopic features promoted the microbial activity in the composites during the soil burial test, leading to their weight loss [28].

In another study, Chee et al. [27] investigated the biodegradability properties of bamboo and kenaf fiber-reinforced epoxy composites. It was reported that the weight loss increased with the increase in fiber loading, exposure time, and soil burial time. In the present study, the outcome of the soil burial degradation test aligns well with that reported

by Chee et al. [27], as with the increase in soil burial time and fiber loading, the weight loss percentage increased.

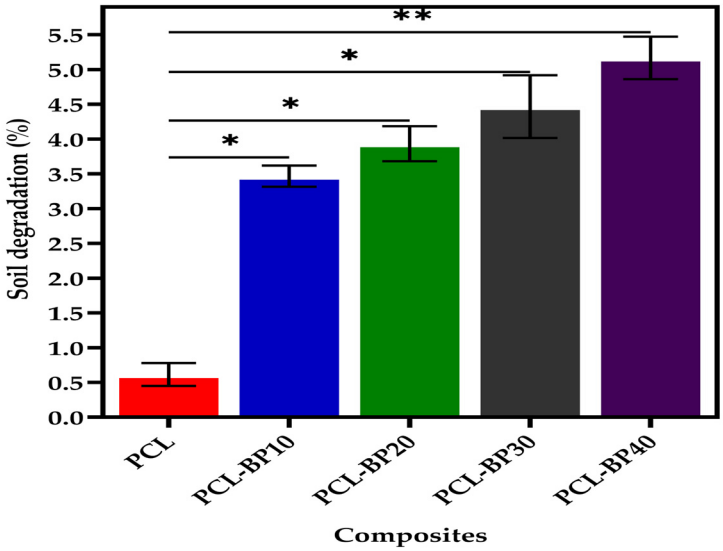

Figure 7. Soil burial degradation of PCL and PCL-BP composites (n = 3, * $p \leq 0.05$, ** $p \leq 0.01$).

3.6. Mechanical Properties

3.6.1. Tensile Properties

Figure 8 presents the tensile stress-strain curves of the PCL and PCL-BP composites. The tensile strength measurements were conducted following those reported by Idicula et al. [58] and Mohanty et al. [59]. The measurements were carried out at 3 mm/min crosshead speed in order to obtain the rupture within the timeframe [60]. Tensile strength was found to increase with the increasing concentration of BP, as reported by Allaf et al. [54]. PCL had a tensile strength of up to 25.82 MPa, whereas PCL-BP10, PCL-BP20, PCL-BP30, and PCL-BP40 exhibited stress concentrations of 28.67, 31.54, 34.12, and 37.27 MPa, respectively. The mechanical properties of the composites are summarized in Table 2, demonstrating that Young's modulus increased with the increase in BP content. According to Bhagabati et al. [10], PCL reinforced with 30% bamboo root flour revealed the highest tensile strength. Similarly, Yang et al. [26] reported that the tensile strength of bamboo fiber-reinforced PP composites increased with the content of fiber. Thus, the addition of BP was sufficient to reinforce the PCL for easy stress transfer and improved tensile strength, as reported in the following literature [61].

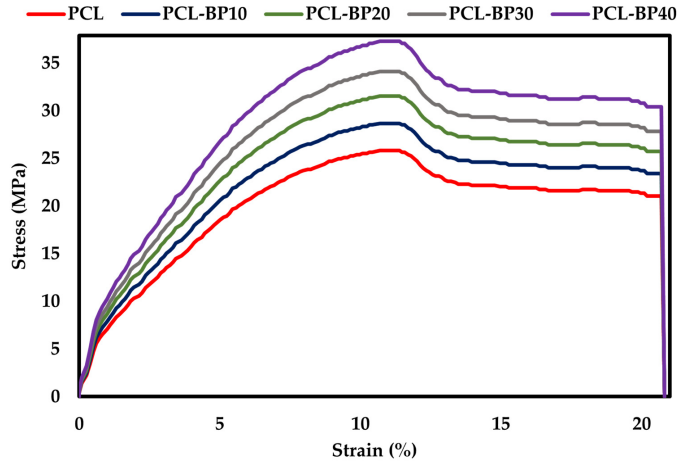

Figure 8. Tensile curve of PCL and PCL-BP composites.

Table 2. Mechanical properties of PCL and PCL-BP composites.

Composite	Young's Modulus (MPa)	Ultimate Tensile Strength (MPa)
PCL	3.01	25.82
PCL-BP10	3.17	28.67
PCL-BP20	3.51	31.54
PCL-BP30	3.92	34.12
PCL-BP40	4.19	37.27

3.6.2. Flexural Properties

The flexural behaviour was measured for the 5% deflection as per the ASTM D790 standard. The PCL-BP composite results were presented in Figure 9. The flexural strength increased with the increase in BP because of the even dispersion of BP in the PCL matrix, as observed in SEM micrographs. The PCL-BP40 had a flexural strength of 17 MPa, while the flexural strengths for the PCL-BP30, PCL-B20, and PCL-B10 were 16 MPa, 14 MPa, and 13 MPa, respectively. The pure PCL had the lowest flexural strength at 12 MPa. Campaña et al. [62] studied the mechanical properties of PLA reinforced with bamboo. It was reported that the 75% PLA and 25% BP composite demonstrated the highest flexural stress and flexural modulus [62]. It was also noted that the flexural strength increased with the increase in filler concentration. The results of the present study are consistent with those of the aforementioned study.

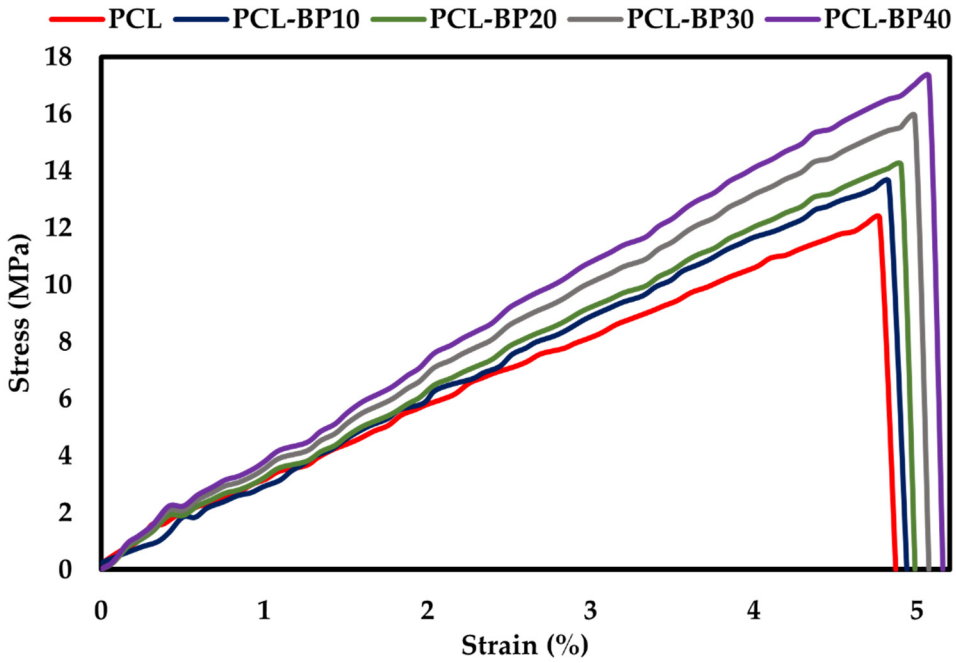

Figure 9. Flexural curves of PCL and PCL-BP composites.

3.7. Hardness

The Vickers microhardness indentation optical images of the PCL-BP composites are shown in Figure 10a–e, and the Vickers hardness values are presented in Figure 10f. The Vickers hardness values significantly increased with the increase in BP. This is consistent with the studies reported by Kaymakci et al. [63] and Kord et al. [64]. A steady increase in the hardness values from PCL-BP10 to PCL-BP40 was observed. The continued rise in hardness values is due to the even dispersion of BP in the PCL matrix and improved interfacial adhesion between the PCL and BP, leading to fewer micro-voids and less filler debonding in the interphase region, which was reported in the following literature by Kaymakci et al. [65]. For instance, PCL had the lowest hardness value (7.2 HV) followed

by PCL-BP10, PCL-BP20, and PCL-BP30 with 8 HV, 8.4 HV, and 9 HV, respectively, and PCL-BP40 had the highest hardness value (9.8 HV). These results are consistent with the study by Jumadi et al. [66].

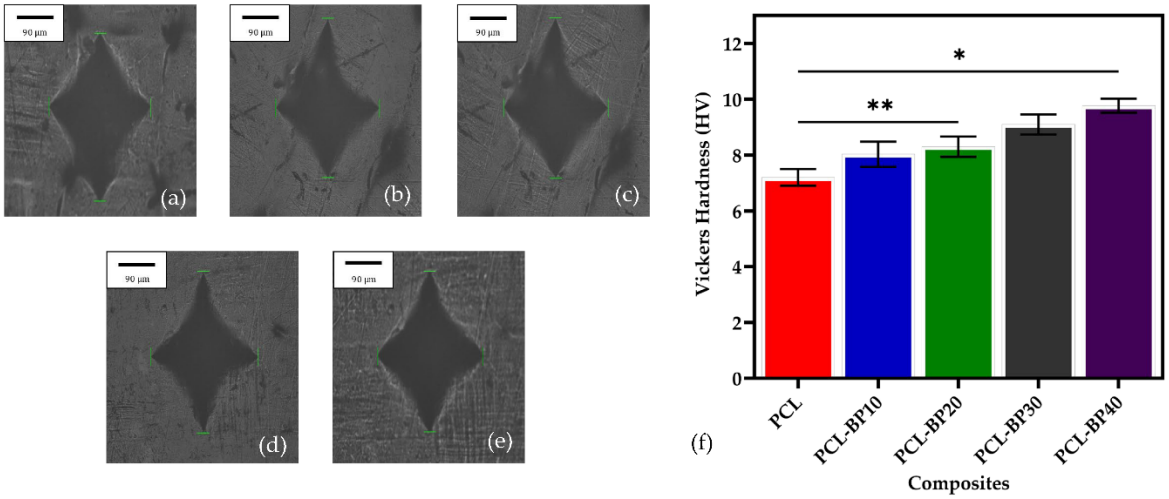

Figure 10. Images of hardness for PCL and PCL-BP composites: (**a**) PCL; (**b**) PCL-BP10; (**c**) PCL-BP20; (**d**) PCL-BP30; (**e**) PCL-BP40; and (**f**) Vickers hardness values (n = 3, * $p \leq 0.05$, ** $p \leq 0.01$).

3.8. Thermal Properties

3.8.1. Thermogravimetric Analysis

The TGA curves of the PCL and PCL-BP composites are presented in Figure 11. The thermal degradation of pure PCL is displayed in a two-step decomposition process. The first step of decomposition occurred at a temperature below 200 °C and was related to the evaporation of moisture in the composites. The second step occurred at a temperature above 350 °C. This second weight loss was associated with the degradation of the main polymer chains of neat PCL. Unlike PCL, the decomposition of PCL-BP occurred in three steps [67]. It was obvious that the first step below 200 °C was associated with the humidity and moisture evaporation from the composites [68]. The second step occurred between 200 and 475 °C and was related to the decomposition of the main components of BP such as cellulose, hemicellulose, and lignin [69–71]. The third step from 480 °C onward to 700 °C was associated with the degradation of residual lignin in PCL-BP composites [72]. The decomposition trends were similar to El Mechtali et al. [73], Rojas-Lema et al. [74], and Açıkalın et al. [75]. At higher temperatures (>500 °C), the presence of carbonated residuals in PCL-BP that were formed due to depolymerization, decomposition, and decarboxylation of hemicellulose and cellulose was noted. Compared to neat PCL, the thermal stability of PCL-BP increased with the addition of BP to the matrix. The thermal stability sequence is as follows: PCL-BP40 > PCLBP30 > PCL-BP20 > PCL-BP10 > PCL. Similar observations were reported for the other wood polymer composites (WPCs) [76,77].

3.8.2. Differential Scanning Calorimetry

The DSC scans of the PCL-BP composites are presented in Figure 12. The enthalpy of melting (ΔH_m) and melting temperature (T_m) of the PCL-BP composites were identified and tabulated in Table 3. It can be seen that T_m increased slightly with the BP content in the PCL matrix. This was mainly caused by the expansion of the BP, which would have loosened the PCL structure as a result of the increased T_m. PCL-BP40 had the highest melting temperature at approximately 57 °C, followed by PCL-BP30, PCL-BP20, and PCL-BP10 at 56 °C, and finally PCL at 55 °C.

The ΔH_m value is used as an indicator of the crystallinity of the composite. The ΔH_m for the PCL-BP composites decreased with the increase in BP content, resulting in a lower degree of crystallinity, as shown in Table 3. These results are similar to those obtained

for BF-reinforced polypropylene composites in the study by Mi et al. [78]. The primary reason for the decrease in the crystallinity of the PCL-BP composites was the hindered motion of the PCL polymer in segments, mainly resulting from the presence of the BP in the composites. This is a result of the steric effect, with PCL being hydrophobic and BP being hydrophilic, leading to good dispersion in the fabrication of composites [46,79]. Similar observations were reported for the other types of WPCs [73,80,81].

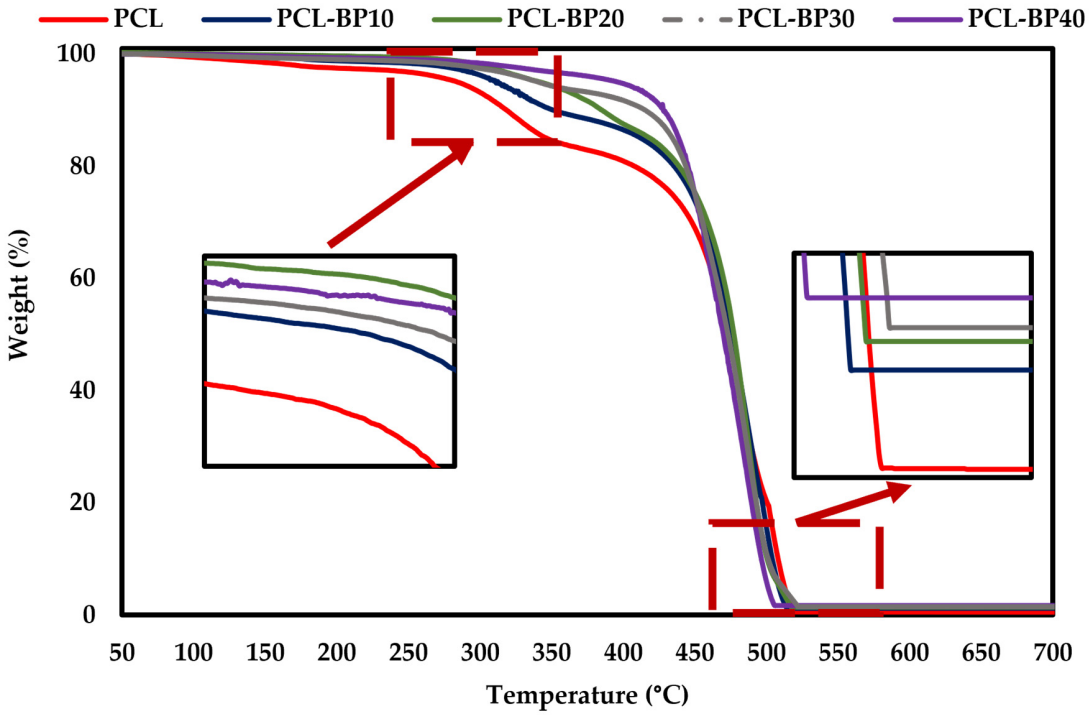

Figure 11. TGA thermograms of PCL and PCL-BP composites.

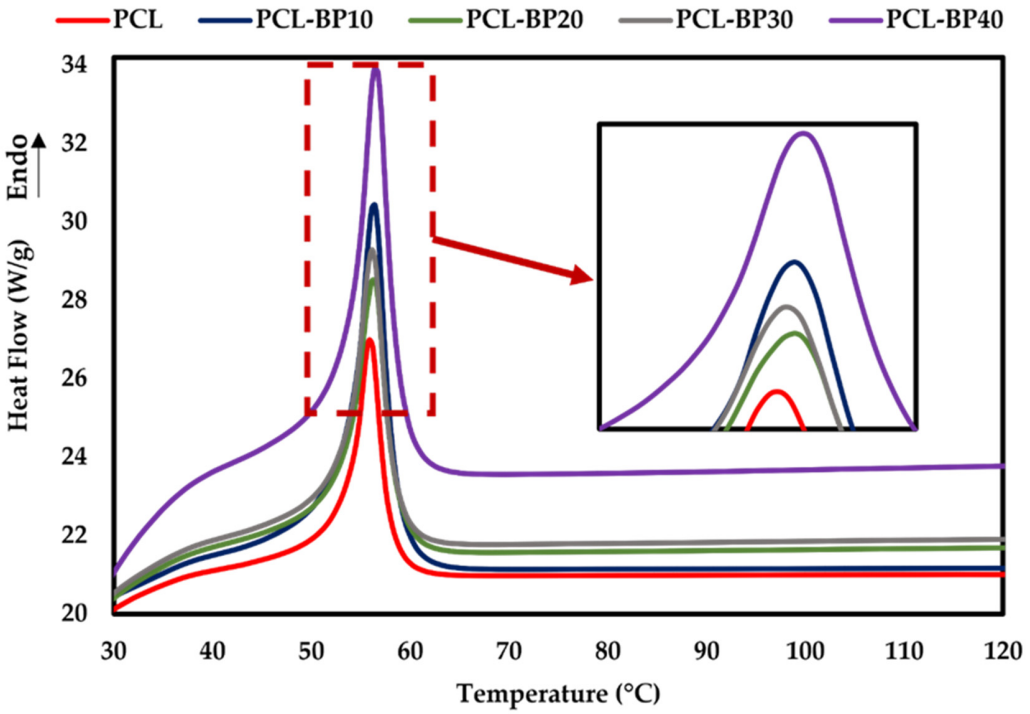

Figure 12. DSC curves of PCL and PCL-BP composites.

Table 3. Melting temperature (T_m) and enthalpy of melting (ΔH_m) of PCL-BP composites.

Sample	Melting Temperature T_m (°C)	Enthalpy of Melting ΔH_m (J/g)
PCL	55	70
PCL-BP10	56	45
PCL-BP20	56	40
PCL-BP30	56	35
PCL-BP40	57	27

4. Conclusions

PCL-BP-reinforced composites were fabricated using solvent casting and compression moulding techniques. The SEM micrographs revealed the even dispersion of PB in the PCL matrix and good interfacial adhesion between the PCL and BP. FTIR results demonstrated that all the individual peaks were related to the PCL-BP composites, indicating no structural changes or chemical bond formations. The biodegradable composites with comparable mechanical properties were obtained, where the tensile strength of the composites increased from 25.82 to 37.27 MPa, and the flexural strength increased from 15 to 23 MPa, with the increase in BP content, highlighting the strength and ductility of the composite with the addition of BP. Furthermore, the hardness of the composites increased from 7 to 9.8 HV with an increase in BP content from 0 wt·% to 40 wt·%. In terms of the thermal properties, it can be noticed that thermal stability increases along with a decrease in decomposition residue, and the melting enthalpy shows a drastic drop from 70 to 25 J/g with the increase in BP content in the PCL-BP composites. The BP content demonstrated the influence of degradation in natural and controlled environments. The degradation of composites increased with the increase in BP, and the degradation rate depended on the number of days. Since BP is hydrophilic in nature, the porosity and wettability increased with the increase in BP concentration (30 and 40 wt·%). The present work demonstrated the development of biodegradable composites with comparable mechanical and thermal properties to synthetic polymer composites, which could be an alternative material to the existing synthetic polymer composites.

Author Contributions: Conceptualization, I.K. and S.G.N.; methodology, S.G.N.; software, S.G.N.; validation, S.G.N., I.K., and A.B.K.; formal analysis, S.G.N. and A.B.K.; investigation, I.K.; resources, I.K.; data curation, S.G.N.; writing—original draft preparation, S.G.N.; writing—review and editing, I.K., W.K., V.I.P., O.B., and A.B.K.; supervision, I.K. and V.I.P. All authors have read and agreed to the published version of the manuscript.

Funding: This research received no external funding.

Institutional Review Board Statement: Not applicable.

Informed Consent Statement: Not applicable.

Data Availability Statement: Not applicable.

Acknowledgments: The authors would like to thank the School of Computing, Engineering and Mathematical Sciences at La Trobe University for supporting this work. The authors also would like to acknowledge Julian Ratcliffe (Bioimaging Platform, La Trobe University) for his kindly aid and valuable inputs on SEM characterisation.

Conflicts of Interest: The authors declare no conflict of interest.

References

1. Goriparthi, B.K.; Suman, K.N.S.; Nalluri, M.R. Processing and characterization of jute fiber reinforced hybrid biocomposites based on polylactide/polycaprolactone blends. *Polym. Compos.* **2012**, *33*, 237–244. [CrossRef]
2. Kakarla, A.B.; Nukala, S.G.; Kong, I. Biodegradable materials. In *Materials for Lightweight Constructions*; CRC Press: Boca Raton, FL, USA, 2022; pp. 161–190.

3. Wu, C.-S. Preparation and characterizations of polycaprolactone/green coconut fiber composites. *J. Appl. Polym. Sci.* **2010**, *115*, 948–956. [CrossRef]
4. Jha, K.; Tyagi, Y.K.; Singh Yadav, A. Mechanical and thermal behaviour of biodegradable composites based on polycaprolactone with pine cone particle. *Sādhanā* **2018**, *43*, 135. [CrossRef]
5. Nukala, S.G.; Kong, I.; Kakarla, A.B.; Tshai, K.Y.; Kong, W. Preparation and Characterisation of Wood Polymer Composites Using Sustainable Raw Materials. *Polymers* **2022**, *14*, 3183. [CrossRef] [PubMed]
6. Abdul Khalil, H.P.S.; Bhat, I.U.H.; Jawaid, M.; Zaidon, A.; Hermawan, D.; Hadi, Y.S. Bamboo fibre reinforced biocomposites: A review. *Mater. Des.* **2012**, *42*, 353–368. [CrossRef]
7. Cintra, S.C.; Braga, N.F.; de Melo Morgado, G.F.; do Amaral Montanheiro, T.L.; Marini, J.; Passador, F.R.; Montagna, L.S. Development of new biodegradable composites materials from polycaprolactone and wood flour. *Wood Mater. Sci. Eng.* **2021**, 1–12. [CrossRef]
8. Chen, Q.; Li, X.; Lin, J. Preparation and properties of biodegradable bamboo powder/ polycaprolactone composites. *J. For. Res.* **2009**, *20*, 271–274. [CrossRef]
9. Labet, M.; Thielemans, W. Synthesis of polycaprolactone: A review. *Chem. Soc. Rev.* **2009**, *38*, 3484. [CrossRef]
10. Bhagabati, P.; Das, D.; Katiyar, V. Bamboo-flour-filled cost-effective poly(ε-caprolactone) biocomposites: A potential contender for flexible cryo-packaging applications. *Mater. Adv.* **2021**, *2*, 280–291. [CrossRef]
11. Si, S.; Tang, Q.; Li, X. The Accelerated Thermo-Oxidative Aging Characteristics of Wood Fiber/Polycaprolactone Composite: Effect of Temperature, Humidity and Time. *J. Renew. Mater.* **2021**, *9*, 2209–2222. [CrossRef]
12. Ilyas, R.A.; Zuhri, M.Y.M.; Norrrahim, M.N.F.; Misenan, M.S.M.; Jenol, M.A.; Samsudin, S.A.; Nurazzi, N.M.; Asyraf, M.R.M.; Supian, A.B.M.; Bangar, S.P.; et al. Natural Fiber-Reinforced Polycaprolactone Green and Hybrid Biocomposites for Various Advanced Applications. *Polymers* **2022**, *14*, 182. [CrossRef] [PubMed]
13. Archer, E.; Torretti, M.; Madbouly, S. Biodegradable polycaprolactone (PCL) based polymer and composites. *Phys. Sci. Rev.* **2021**. [CrossRef]
14. Karakus, K. Polycaprolactone (PCL) based polymer composites filled wheat straw flour. *Kastamonu Üniversitesi Orman Fakültesi Derg.* **2016**, *16*. [CrossRef]
15. Valdés, A.; Fenollar, O.; Beltrán, A.; Balart, R.; Fortunati, E.; Kenny, J.M.; Garrigós, M.C. Characterization and enzymatic degradation study of poly(ε-caprolactone)-based biocomposites from almond agricultural by-products. *Polym. Degrad. Stab.* **2016**, *132*, 181–190. [CrossRef]
16. Kitagawa, K.; Shimamura, T.; Senba, K.; Okumura, H.; Takasima, S.; Hamaguchi, M.; Nakai, A.; Hamada, H.; Lee, S.H.; Ohkita, T. Development of bamboo fiber-reinforced biodegradable polymer composites. *Jpn. Soc. Polym. Process.* **2003**, *3*, 165–166.
17. Okubo, K.; Fujii, T.; Yamamoto, Y. Development of bamboo-based polymer composites and their mechanical properties. *Compos. Part A Appl. Sci. Manuf.* **2004**, *35*, 377–383. [CrossRef]
18. Radzi, A.M.; Zaki, S.A.; Hassan, M.Z.; Ilyas, R.A.; Jamaludin, K.R.; Daud, M.Y.M.; Aziz, S.A. Bamboo-Fiber-Reinforced Thermoset and Thermoplastic Polymer Composites: A Review of Properties, Fabrication, and Potential Applications. *Polymers* **2022**, *14*, 1387. [CrossRef]
19. Nkeuwa, W.N.; Zhang, J.; Semple, K.E.; Chen, M.; Xia, Y.; Dai, C. Bamboo-based composites: A review on fundamentals and processes of bamboo bonding. *Compos. Part B Eng.* **2022**, *235*, 109776. [CrossRef]
20. Rasheed, M.; Jawaid, M.; Parveez, B.; Hussain Bhat, A.; Alamery, S. Morphology, Structural, Thermal, and Tensile Properties of Bamboo Microcrystalline Cellulose/Poly(Lactic Acid)/Poly(Butylene Succinate) Composites. *Polymer* **2021**, *13*, 465. [CrossRef]
21. Zhao, X.; Jin, Y.; Zhu, X.; Zhu, L. Effect of Bamboo Fiber Mass Fraction on Properties of PCL/PLA/Bamboo Fiber Composites. *Plast. Sci. Technol.* **2016**, 10.
22. Zhang, Y.-C.; Wu, H.-Y.; Qiu, Y.-P. Morphology and properties of hybrid composites based on polypropylene/polylactic acid blend and bamboo fiber. *Bioresour. Technol.* **2010**, *101*, 7944–7950. [CrossRef]
23. Qi, W.; Taherzadeh, M.J.; Ruan, Y.; Deng, Y.; Chen, J.-S.; Lu, H.-F.; Xu, X.-Y. Denitrification performance and microbial communities of solid-phase denitrifying reactors using poly (butylene succinate)/bamboo powder composite. *Bioresour. Technol.* **2020**, *305*, 123033. [CrossRef] [PubMed]
24. Kieling, A.C.; Santana, G.P.; Dos Santos, M.D.D.M.C.; Neto, J.C.D.M.; Del Pino, G.G.; Dos Santos, M.D.D.M.C.; Duvoisin, S.; Panzera, T.H. Wood-plastic Composite Based on Recycled Polypropylene and Amazonian Tucumã (*Astrocaryum aculeatum*) Endocarp Waste. *Fibers Polym.* **2021**, *22*, 2834–2845. [CrossRef]
25. Tiwari, S.K.; Umamaheswara Rao, A.; Reddy, N.; Sharma, H.; Pandey, J.K. Synthesis, characterization and finite element analysis of polypropylene composite reinforced by jute and carbon fiber. *Mater. Today Proc.* **2021**. [CrossRef]
26. Yang, F.; Long, H.; Xie, B.; Zhou, W.; Luo, Y.; Zhang, C.; Dong, X. Mechanical and biodegradation properties of bamboo fiber-reinforced starch/polypropylene biodegradable composites. *J. Appl. Polym. Sci.* **2020**, *137*, 48694. [CrossRef]
27. Chee, S.S.; Jawaid, M.; Sultan, M.T.H.; Alothman, O.Y.; Abdullah, L.C. Accelerated weathering and soil burial effects on colour, biodegradability and thermal properties of bamboo/kenaf/epoxy hybrid composites. *Polym. Test.* **2019**, *79*, 106054. [CrossRef]
28. Maran, J.P.; Sivakumar, V.; Thirugnanasambandham, K.; Sridhar, R. Degradation behavior of biocomposites based on cassava starch buried under indoor soil conditions. *Carbohydr. Polym.* **2014**, *101*, 20–28. [CrossRef]
29. Kakarla, A.B.; Kong, I.; Turek, I.; Kong, C.; Irving, H. Printable gelatin, alginate and boron nitride nanotubes hydrogel-based ink for 3D bioprinting and tissue engineering applications. *Mater. Des.* **2022**, *213*, 110362. [CrossRef]

30. Johari, N.; Fathi, M.H.; Golozar, M.A. Fabrication, characterization and evaluation of the mechanical properties of poly (ε-caprolactone)/nano-fluoridated hydroxyapatite scaffold for bone tissue engineering. *Compos. Part B Eng.* **2012**, *43*, 1671–1675. [CrossRef]
31. Sdrobiş, A.; Darie, R.N.; Totolin, M.; Cazacu, G.; Vasile, C. Low density polyethylene composites containing cellulose pulp fibers. *Compos. Part B Eng.* **2012**, *43*, 1873–1880. [CrossRef]
32. Wang, P.; Liang, C.; Wu, B.; Huang, N.; Li, J. Protection of copper corrosion by modification of dodecanethiol self-assembled monolayers prepared in aqueous micellar solution. *Electrochim. Acta* **2010**, *55*, 878–883. [CrossRef]
33. Li, Y.-F.; Liu, Y.-X.; Wang, X.-M.; Wu, Q.-L.; Yu, H.-P.; Li, J. Wood-polymer composites prepared by the in situ polymerization of monomers within wood. *J. Appl. Polym. Sci.* **2011**, *119*, 3207–3216. [CrossRef]
34. Prabhakar, M.N.; ur Rehman Shah, A.; Song, J.-I. Improved flame-retardant and tensile properties of thermoplastic starch/flax fabric green composites. *Carbohydr. Polym.* **2017**, *168*, 201–211. [CrossRef]
35. Li, Z.; Wang, L.; Wang, X. Compressive and flexural properties of hemp fiber reinforced concrete. *Fibers Polym.* **2004**, *5*, 187–197. [CrossRef]
36. Li, Z.; Wang, X.; Wang, L. Properties of hemp fibre reinforced concrete composites. *Compos. Part A Appl. Sci. Manuf.* **2006**, *37*, 497–505. [CrossRef]
37. Okonkwo, E.G.; Anabaraonye, C.N.; Daniel-Mkpume, C.C.; Egoigwe, S.V.; Okeke, P.E.; Whyte, F.G.; Okoani, A.O. Mechanical and thermomechanical properties of clay-Bambara nut shell polyester bio-composite. *Int. J. Adv. Manuf. Technol.* **2020**, *108*, 2483–2496. [CrossRef]
38. Nukala, S.G.; Kong, I.; Kakarla, A.B.; Kong, W.; Kong, W. Development of Wood Polymer Composites from Recycled Wood and Plastic Waste: Thermal and Mechanical Properties. *J. Compos. Sci.* **2022**, *6*, 194. [CrossRef]
39. Kakarla, A.B.; Kong, I.; Kong, C.; Irving, H. Extrusion-Based Bioprinted Boron Nitride Nanotubes Reinforced Alginate Scaffolds: Mechanical, Printability and Cell Viability Evaluation. *Polymers* **2022**, *14*, 486. [CrossRef]
40. da Silva, W.A.; Luna, C.B.B.; da Costa Agra de Melo, J.B.; Araújo, E.M.; dos S. Filho, E.A.; Duarte, R.N.C. Feasibility of Manufacturing Disposable Cups using PLA/PCL Composites Reinforced with Wood Powder. *J. Polym. Environ.* **2021**, *29*, 2932–2951. [CrossRef]
41. Shibata, M.; Inoue, Y.; Miyoshi, M. Mechanical properties, morphology, and crystallization behavior of blends of poly(l-lactide) with poly(butylene succinate-co-l-lactate) and poly(butylene succinate). *Polymer* **2006**, *47*, 3557–3564. [CrossRef]
42. Hernández, A.R.; Contreras, O.C.; Acevedo, J.C.; Moreno, L.G.N. Poly (ε-caprolactone) degradation under acidic and alkaline conditions. *Am. J. Polym. Sci* **2013**, *3*, 70–75.
43. Lyu, J.S.; Lee, J.-S.; Han, J. Development of a biodegradable polycaprolactone film incorporated with an antimicrobial agent via an extrusion process. *Sci. Rep.* **2019**, *9*, 20236. [CrossRef] [PubMed]
44. Hoidy, H.W.; Ahmad, B.M.; Almulla, E.; Ibrahim, N.A. Preparation and Characterization of Polylactic Acid/Polycaprolactone Clay Nanocomposites. *J. Appl. Sci.* **2010**, *10*, 97–106. [CrossRef]
45. Hejna, A.; Piszcz-Karaś, K.; Filipowicz, N.; Cieśliński, H.; Namieśnik, J.; Marć, M.; Klein, M.; Formela, K. Structure and performance properties of environmentally-friendly biocomposites based on poly(ε-caprolactone) modified with copper slag and shale drill cuttings wastes. *Sci. Total Environ.* **2018**, *640–641*, 1320–1331. [CrossRef]
46. Su, S.-K.; Wu, C.-S. The Processing and Characterization of Polyester/Natural Fiber Composites. *Polym. Plast. Technol. Eng.* **2010**, *49*, 1022–1029. [CrossRef]
47. Liew, F.K.; Hamdan, S.; Rahman, M.R.; Mahmood, M.R.; Lai, J.C.H. The effects of nanoclay and tin(IV) oxide nanopowder on morphological, thermo-mechanical properties of hexamethylene diisocyanate treated jute/bamboo/polyethylene hybrid composites. *J. Vinyl Addit. Technol.* **2018**, *24*, 358–366. [CrossRef]
48. Elzein, T.; Nasser-Eddine, M.; Delaite, C.; Bistac, S.; Dumas, P. FTIR study of polycaprolactone chain organization at interfaces. *J. Colloid Interface Sci.* **2004**, *273*, 381–387. [CrossRef]
49. Vidal, J.L.; Yavitt, B.M.; Wheeler, M.D.; Kolwich, J.L.; Donovan, L.N.; Sit, C.S.; Hatzikiriakos, S.G.; Jalsa, N.K.; MacQuarrie, S.L.; Kerton, F.M. Biochar as a sustainable and renewable additive for the production of Poly(ε-caprolactone) composites. *Sustain. Chem. Pharm.* **2022**, *25*, 100586. [CrossRef]
50. Swain, P.T.R.; Biswas, S. A comparative analysis of physico-mechanical, water absorption, and morphological behaviour of surface modified woven jute fiber composites. *Polym. Compos.* **2018**, *39*, 2952–2960. [CrossRef]
51. Panthapulakkal, S.; Sain, M. Injection-molded short hemp fiber/glass fiber-reinforced polypropylene hybrid composites—Mechanical, water absorption and thermal properties. *J. Appl. Polym. Sci.* **2007**, *103*, 2432–2441. [CrossRef]
52. Büyüksarı, Ü.; Avci, E.; Akkılıç, H. Effect of pine cone ratio on the wettability and surface roughness of particleboard. *Bioresources* **2014**, *5*, 1824–1833.
53. Borysiuk, P.; Wilkowski, J.; Krajewski, K.; Auriga, R.; Skomorucha, A.; Auriga, A. Selected properties of flat-pressed wood-polymer composites for high humidity conditions. *BioResources* **2020**, *15*, 5141–5155. [CrossRef]
54. Allaf, R.M.; Futian, M. Solid-State Compounding for Recycling of Sawdust Waste into Green Packaging Composites. *Processes* **2020**, *8*, 1386. [CrossRef]
55. Wu, C.-S.; Wu, D.-Y.; Wang, S.-S. Preparation and Characterization of Polylactic Acid/Bamboo Fiber Composites. *ACS Appl. Bio Mater.* **2022**, *5*, 1038–1046. [CrossRef]

56. Dinesh, S.; Kumaran, P.; Mohanamurugan, S.; Vijay, R.; Singaravelu, D.L.; Vinod, A.; Sanjay, M.R.; Siengchin, S.; Bhat, K.S. Influence of wood dust fillers on the mechanical, thermal, water absorption and biodegradation characteristics of jute fiber epoxy composites. *J. Polym. Res.* **2020**, *27*, 9. [CrossRef]
57. Schirp, A.; Ibach, R.E.; Pendleton, D.E.; Wolcott, M.P. Biological Degradation of Wood-Plastic Composites (WPC) and Strategies for Improving the Resistance of WPC against Biological Decay. In *Development of Commercial Wood Preservatives*; American Chemical Society: Washington, DC, USA, 2008; pp. 480–507.
58. Idicula, M.; Malhotra, S.K.; Joseph, K.; Thomas, S. Dynamic mechanical analysis of randomly oriented intimately mixed short banana/sisal hybrid fibre reinforced polyester composites. *Compos. Sci. Technol.* **2005**, *65*, 1077–1087. [CrossRef]
59. Mohanty, A.K.; Khan, M.A.; Hinrichsen, G. Influence of chemical surface modification on the properties of biodegradable jute fabrics—polyester amide composites. *Compos. Part A Appl. Sci. Manuf.* **2000**, *31*, 143–150. [CrossRef]
60. Sood, A.; Ramarao, S.; Carounanidy, U. Influence of different crosshead speeds on diametral tensile strength of a methacrylate based resin composite: An in-vitro study. *J. Conserv. Dent.* **2015**, *18*, 214. [CrossRef]
61. Krishnaprasad, R.; Veena, N.R.; Maria, H.J.; Rajan, R.; Skrifvars, M.; Joseph, K. Mechanical and Thermal Properties of Bamboo Microfibril Reinforced Polyhydroxybutyrate Biocomposites. *J. Polym. Environ.* **2009**, *17*, 109. [CrossRef]
62. Campaña, O.; Guerrero, V.H. Mechanical and Thermal Characterization of Polylactic Acid (PLA) Reinforced with Bamboo Powder (PB). *Rev. Politécnica* **2018**, *42*, 17–24.
63. Kaymakci, A.; Ayrilmis, N.; Gulec, T. Surface properties and hardness of polypropylene composites filled with sunflower stalk flour. *BioResources* **2013**, *8*, 592–602. [CrossRef]
64. Kord, B. Investigation of reinforcing filler loading on the mechanical properties of wood plastic composites. *World Appl. Sci. J.* **2011**, *13*, 171–174.
65. Kaymakci, A.; Ayrilmis, N. Investigation of correlation between Brinell hardness and tensile strength of wood plastic composites. *Compos. Part B Eng.* **2014**, *58*, 582–585. [CrossRef]
66. Jumadi, M.T.; Mansor, M.R.; Mustafa, Z.; Tokoroyama, T.; Umehara, N. The study on microhardness of natural fibre composite made by recycled material. In Proceedings of the SAKURA Symposium on Mechanical Science and Engineering 2017, Nagoya, Japan, 12 September 2017.
67. Norizan, M.N.; Abdan, K.; Salit, M.S.; Mohamed, R. Physical, mechanical and thermal properties of sugar palm yarn fibre loading on reinforced unsaturated polyester composites. *J. Phys. Sci.* **2017**, *28*. [CrossRef]
68. Monteiro, S.N.; Calado, V.; Rodriguez, R.J.S.; Margem, F.M. Thermogravimetric behavior of natural fibers reinforced polymer composites—An overview. *Mater. Sci. Eng. A* **2012**, *557*, 17–28. [CrossRef]
69. Kumar, A.; Wang, L.; Dzenis, Y.A.; Jones, D.D.; Hanna, M.A. Thermogravimetric characterization of corn stover as gasification and pyrolysis feedstock. *Biomass Bioenergy* **2008**, *32*, 460–467. [CrossRef]
70. Mansaray, K.G.; Ghaly, A.E. Thermal degradation of rice husks in nitrogen atmosphere. *Bioresour. Technol.* **1998**, *65*, 13–20. [CrossRef]
71. Youssefian, S.; Rahbar, N. Molecular Origin of Strength and Stiffness in Bamboo Fibrils. *Sci. Rep.* **2015**, *5*, 11116. [CrossRef] [PubMed]
72. Kaymakci, A.; Gulec, T.; Hosseinihashemi, S.K.; Ayrilmis, N. Physical, mechanical and thermal properties of wood/zeolite/plastic hybrid composites. *Maderas. Cienc. Tecnol.* **2017**. [CrossRef]
73. El Mechtali, F.Z.; Essabir, H.; Nekhlaoui, S.; Bensalah, M.O.; Jawaid, M.; Bouhfid, R.; Qaiss, A. Mechanical and thermal properties of polypropylene reinforced with almond shells particles: Impact of chemical treatments. *J. Bionic Eng.* **2015**, *12*, 483–494. [CrossRef]
74. Rojas-Lema, S.; Arevalo, J.; Gomez-Caturla, J.; Garcia-Garcia, D.; Torres-Giner, S. Peroxide-Induced Synthesis of Maleic Anhydride-Grafted Poly(butylene succinate) and Its Compatibilizing Effect on Poly(butylene succinate)/Pistachio Shell Flour Composites. *Molecules* **2021**, *26*, 5927. [CrossRef] [PubMed]
75. Açıkalın, K. Thermogravimetric analysis of walnut shell as pyrolysis feedstock. *J. Therm. Anal. Calorim.* **2011**, *105*, 145–150. [CrossRef]
76. Lei, Y.; Wu, Q.; Yao, F.; Xu, Y. Preparation and properties of recycled HDPE/natural fiber composites. *Compos. Part A Appl. Sci. Manuf.* **2007**, *38*, 1664–1674. [CrossRef]
77. Satapathy, S.; Kothapalli, R.V.S. Mechanical, Dynamic Mechanical and Thermal Properties of Banana Fiber/Recycled High Density Polyethylene Biocomposites Filled with Flyash Cenospheres. *J. Polym. Environ.* **2018**, *26*, 200–213. [CrossRef]
78. Mi, Y.; Chen, X.; Guo, Q. Bamboo fiber-reinforced polypropylene composites: Crystallization and interfacial morphology. *J. Appl. Polym. Sci.* **1997**, *64*, 1267–1273. [CrossRef]
79. Prinos, J.; Bikiaris, D.; Theologidis, S.; Panayiotou, C. Preparation and characterization of LDPE/starch blends containing ethylene/vinyl acetate copolymer as compatibilizer. *Polym. Eng. Sci.* **1998**, *38*, 954–964. [CrossRef]
80. Salazar-Cruz, B.A.; Chávez-Cinco, M.Y.; Morales-Cepeda, A.B.; Ramos-Galván, C.E.; Rivera-Armenta, J.L. Evaluation of Thermal Properties of Composites Prepared from Pistachio Shell Particles Treated Chemically and Polypropylene. *Molecules* **2022**, *27*, 426. [CrossRef]
81. Huang, Y.; Liu, H.; He, P.; Yuan, L.; Xiong, H.; Xu, Y.; Yu, Y. Nonisothermal crystallization kinetics of modified bamboo fiber/PCL composites. *J. Appl. Polym. Sci.* **2010**, *116*, 2119–2125. [CrossRef]